

FEDERATED FEATURE TRANSFORMATION WITH SAMPLE-AWARE CALIBRATION AND LOCAL–GLOBAL SEQUENCE FUSION

000
001
002
003
004
005
006
007 **Anonymous authors**
008 Paper under double-blind review
009
010
011
012

ABSTRACT

013 Tabular data plays a crucial role in numerous real-world decision-making applica-
014 tions, but extracting valuable insights often requires sophisticated feature trans-
015 formations. These transformations mathematically transform raw data, signifi-
016 cantly improving predictive performance. In practice, tabular datasets are fre-
017 quently fragmented across multiple clients due to widespread data distribution,
018 privacy restrictions, and data silos, making it challenging to derive unified and
019 generalized insights. To address them, we propose a Federated Feature Transfor-
020 mation (FEDFT) framework that enables collaborative learning while preserving
021 data privacy. In this framework, each local client independently computes feature
022 transformation sequences and evaluates the corresponding model performances.
023 Instead of exchanging sensitive original data, clients transmit these transforma-
024 tion sequences and performance metrics to a central global server. The server
025 then compresses and encodes the aggregated knowledge into a unified embedding
026 space, facilitating the identification of optimal feature transformation sequences.
027 To ensure unbiased aggregation, we tackle three challenges in distributed tabular
028 data: insufficient samples compromise statistics, limited feature diversity misses
029 patterns, and sparse or correlated columns cause instability. We employ a sample-
030 aware weighting strategy that favors clients with adequate size, rich diversity, and
031 stable numerical properties. We also incorporate a server-side calibration mecha-
032 nism to adaptively refine the unified embedding space, mitigating bias from out-
033 lier data distributions. Furthermore, to ensure optimal transformation sequences
034 at both global and local scales, the globally optimal sequences are disseminated
035 back to local clients. We subsequently develop a sequence fusion strategy that
036 blends these globally optimal features with essential non-overlapping local trans-
037 formations critical for local predictions. Extensive experiments are conducted to
038 demonstrate the efficiency, effectiveness, and robustness of our framework. Code
039 and data are publicly available.¹.
040

1 INTRODUCTION

041 Tabular data is ubiquitous across diverse domains and serves as a fundamental backbone for real-
042 world decision-making applications. To facilitate insight extraction and enhance model perfor-
043 mance, feature transformation systematically applies mathematical operations to raw features, pro-
044 ducing more expressive and informative features. In real-world scenarios, tabular data is often dis-
045 tributed across multiple local clients, resulting in isolated data silos. Due to privacy and regulatory
046 constraints, it becomes challenging to derive unified and generalizable insights from such frag-
047 mented sources. Overcoming these limitations imposed by data silos and achieving unified modeling
048 of tabular data across diverse regions has emerged as a critical and active research direction. Existing
049 works on feature transformation predominantly focus on centralized settings, assuming datasets
050 reside on a single machine, thereby enabling these methods to utilize the complete feature space for
051 effective refinement. They can be mainly classified into three categories: 1) Expansion reduction
052 methods Horn et al. (2019); Khurana et al. (2016) generate numerous candidate features via mathe-
053

¹https://anonymous.4open.science/r/FedFT_ICLR2026-3578

054 matical transformations, subsequently selecting the most informative subset; 2) Iterative feedback-
 055 based techniques: Khurana et al. (2018); Tran et al. (2016); Wang et al. (2022) progressively refine
 056 features using predictive performance feedback, typically optimized through reinforcement learning
 057 or evolutionary algorithms; 3) AutoML-driven frameworks Chen et al. (2019); Zhu et al. (2022);
 058 Wang et al. (2023) formalize feature transformation as neural architecture or policy search problems,
 059 aiming to identify optimal feature transformation sequences to enhance task-specific performance.
 060 But, due to centralized learning constraints, these methods are unable to aggregate knowledge from
 061 multiple clients, limiting their capability to derive unified and generalized feature insights.

062 To address these limitations, we propose a unified automated feature transformation framework ca-
 063 pable of aggregating knowledge from diverse clients and deriving an optimal feature transformation
 064 sequence. Given the distributed nature of data across multiple clients and concerns about privacy,
 065 Federated Learning (FL) naturally emerges as a suitable paradigm, allowing collaborative learning
 066 without compromising local data confidentiality McMahan et al. (2017); Li et al. (2020); Karim-
 067 ireddy et al. (2020). However, adopting FL in this context introduces three major challenges:

- 068 • **Privacy-Preserving Globally Optimal Feature Transformation.** Learning globally op-
 069 timal feature transformation sequences from distributed tabular data presents privacy chal-
 070 lenges. In domains such as healthcare, tabular datasets often contain sensitive information,
 071 including treatment histories, personal demographics, and etc. Transmitting such data
 072 across clients introduces serious privacy risks. Thus, it is essential to develop mechanisms
 073 that support effective knowledge aggregation while strictly preserving data privacy.
- 074 • **Unbiased Aggregation under Non-IID and Imbalanced Distributions.** Client data ex-
 075 hibit heterogeneity in both feature distributions and sample sizes. Such disparity poses a
 076 unique challenge when aggregating feature transformation knowledge, as it can introduce
 077 bias into the global embedding space. This bias may lead to suboptimal transformation
 078 sequences and reduced feature space quality. Thus, it is critical to design aggregation
 079 strategies that explicitly account for data imbalance and distributional shifts across clients.
- 080 • **Effective Feedback from Global Server to Local Clients.** Ensuring that local clients
 081 benefit from global knowledge is crucial for sustainable collaboration. For instance, in
 082 financial applications, institutions may be reluctant to participate if they contribute data but
 083 receive no benefits. Thus, it is necessary to develop feedback mechanisms that adapt global
 084 transformation sequences to local contexts, promoting mutual benefit in this scenario.

085 To address these challenges, we propose a novel **FEDerated Feature Transformation** framework
 086 (**FEDFT**), which enables collaborative feature transformation across clients while preserving data
 087 privacy. The primary objective of FEDFT is to construct an optimized and generalizable feature
 088 space by aggregating transformation knowledge from heterogeneous local datasets without expos-
 089 ing raw data. Specifically, each client independently generates a collection of feature transformation
 090 records, where each record comprises a transformation sequence and associated performance, eval-
 091 uated on the client’s local tabular data. These records are then transmitted to a global central server for
 092 global knowledge aggregation. Notably, only the transformation sequences and corresponding pre-
 093 dictive performance are shared, ensuring that sensitive raw data remains local and protected through-
 094 out the process. To effectively compress and leverage the collected transformation knowledge, we
 095 design an encoder-decoder-evaluator architecture. The encoder maps transformation sequences into
 096 a shared latent embedding space, the decoder reconstructs the sequences from their embeddings, and
 097 the evaluator estimates the expected model performance from the latent representation. Once the
 098 embedding space is constructed, we utilize gradient signals from the evaluator to guide exploration
 099 within the space, enabling the discovery of improved feature transformation sequences. To ensure
 100 unbiased aggregation throughout the optimization process, we introduce a sample-aware weight-
 101 ing mechanism that accounts for the varying reliability of transformation records across clients.
 102 Specifically, in tabular data contexts, we prioritize clients based on three factors: sample size for
 103 statistical validity, feature diversity for comprehensive pattern coverage, and numerical stability for
 104 robust metrics. This is complemented by a server-side calibration process to further mitigate bias
 105 from outlier distributions. To support both global generalization and local adaptability, the globally
 106 optimized transformation sequences are fed back to individual clients. We then develop a sequence
 107 fusion strategy that integrates these global sequences with critical, non-overlapping local transfor-
 108 mations tailored to the specific predictive needs of each client. Finally, we conduct comprehensive
 109 experiments to validate the effectiveness, generalizability, and practical utility of the framework.

108

2 RELATED WORKS

109
 110 **Automated Feature Transformation (AFT)** aims to refine or augment the original feature space so
 111 that machine learning models can more effectively capture complex, high-order relationships among
 112 variables. Most AutoML pipelines refine the input space in one of two ways: (i) by applying explicit
 113 statistical or arithmetic operators to create interpretable composite features Horn et al. (2019); Kan-
 114 ter & Veeramachaneni (2015); Khurana et al. (2016; 2018); Tran et al. (2016); Wang et al. (2022);
 115 Chen et al. (2019); Zhu et al. (2022); Wang et al. (2023), or (ii) by learning high-dimensional la-
 116 tent representations, where feature interactions are implicitly captured through deep representation
 117 learning Bengio et al. (2013); Guo et al. (2017). Despite their effectiveness, both methods assume
 118 centralized access to the full dataset, and latent approaches further obscure provenance, reducing
 119 interpretability—constraints that render them unsuitable for privacy-constrained FL settings.
 120

121 **Federated Learning (FL)** In FL settings, a central server orchestrates multiple clients by aggregat-
 122 ing locally-computed model updates (gradients or weights) over communication rounds, keeping
 123 raw data on-device McMahan et al. (2017). Consequently, classical FL research has focused on
 124 parameter-level aggregation for prediction tasks, proposing algorithms like FedAvg McMahan et al.
 125 (2017), FedProx Li et al. (2020), and SCAFFOLD Karimireddy et al. (2020) to address system and
 126 statistical heterogeneity. However, these methods have rarely been extended to feature transfor-
 127 mation workflows. Existing FL variants that manipulate features operate only in the latent space—e.g.,
 128 by mixing, aligning, or augmenting embeddings Yoon et al. (2021); Shin et al. (2020); Rasouli et al.
 129 (2020), and fall short of producing explicit, interpretable feature constructions. Adapting centralized
 130 AutoFE to FL remains challenging: combinatorial candidate search leads to excessive cross-device
 131 evaluations, increasing communication and compute costs, and most pipelines entwine feature trans-
 132 formation with iterative model feedback, making most approaches inefficient or impractical to adapt.
 133

134 Research on combining FL and AFT remains limited despite advances in both fields. While prior
 135 studies have explored privacy-preserving **feature selection** via methods like gradient masking, se-
 136 cure aggregation, or differential privacy Zhang et al. (2023); Cassará et al. (2022); Fu et al. (2023),
 137 **feature transformation** remains overlooked due to its combinatorial search space, which ampli-
 138 fies communication and privacy challenges. To our knowledge, FLFE Fang et al. (2020) is the
 139 first framework for federated feature transformation(FFT). It relies on manually defined operators,
 140 scales poorly with growing candidates, and only filters features rather than synthesizing new ones.
 141 Recent work, Fed-IIFE Overman & Klabjan (2024) requires uniform local models across clients
 142 and server, restricts its evaluation loop to pairwise interactions, limiting scalability and higher-order
 143 dependency modeling. Unlike existing methods built on model-level fusion, FEDFT optimizes at
 144 the data level by encoding local feature transformation sequences in a shared latent space. Through
 145 an encoder-decoder-evaluator architecture, it compresses and refines transformation knowledge for
 146 effective inference, cross-client integration, and scalability. Notably, FEDFT enables bi-directional
 147 optimization between local and global spaces, offering a novel and effective approach to FFT.
 148

149

3 PRELIMINARIES

150 **Feature Transformation Sequence.** Feature transformation enhances the tabular feature space by
 151 applying mathematical operations to original features. Given a feature space $[f_1, f_2, \dots, f_N]$, we
 152 define each transformation as a mathematical composition over features and operations. For ex-
 153 ample, one generated feature is $(f_1 + \frac{f_1 - f_2}{f_3} - f_2)$, where f_1, f_2, f_3 are original features and $+, -, /$
 154 are operations. We adopt the postfix expression encoding from Wang et al. (2023) to represent the
 155 entire feature transformation sequence as $\Upsilon = [\gamma_1, \gamma_2, \dots, \gamma_M]$, where each γ_i is a feature index
 156 token or an operation. This sequence guides the construction of a more expressive feature space.
 157

158 **Problem Statement.** Our objective is to develop a novel federated feature transformation framework
 159 that constructs an optimized generalizable feature space by aggregating transformation knowledge
 160 from heterogeneous local tabular data without sharing raw data. Formally, for a tabular data predic-
 161 tion task, each client holds its own local data set $\mathcal{D} = \{\mathbf{X}, \mathbf{y}\}$, where \mathbf{X} is the feature set and \mathbf{y} is
 162 the predictive target. Each client initially generates a set of feature transformation records, denoted
 163 as $\mathcal{R} = \{\Upsilon, \mathbf{v}\}$, where Υ represents the collection of transformation sequences and \mathbf{v} denotes the
 164 corresponding predictive performances. The records of different clients are uploaded to a central
 165 server for subsequent knowledge aggregation. On the server, an encoder ϕ , decoder ψ , and evalua-
 166 tor ω are jointly trained to embed the feature transformation knowledge from the collected records
 167

162 into a continuous space \mathcal{E} . After training, the optimal global transformation sequence is identified
 163 by performing a gradient-based search in the embedding space \mathcal{E} to maximize the weighted average
 164 performance across all clients: $\Upsilon^* = \arg \max_{\Upsilon \in \psi(\mathcal{E})} \sum_{k=1}^K w_k v_k$, where w_k denotes the weight of
 165 client k , and v_k denotes the predicted performance on client k for the feature space generated by Υ .
 166

167 4 METHODOLOGY

168 4.1 FRAMEWORK OVERVIEW OF FEDERATED FEATURE TRANSFORMATION

169 Figure 1 presents the complete FEDFT workflow. Each client first explores its local tabular
 170 dataset using an RL-based collector, generating
 171 a set of feature transformation records. These
 172 records, together with the corresponding sam-
 173 ple metrics, are uploaded to the server. On the
 174 server side, records from all clients are merged
 175 using a sample-aware weighting scheme to pro-
 176 duce an unbiased, population-level estimate for
 177 each transformation sequence. The aggregated
 178 sequence–performance pairs are then used to
 179 train an encoder–decoder–evaluator network,
 180 which projects the sequences into a shared la-
 181 tent space while learning to predict their per-
 182 formance. After the model converges, a gradient-
 183 guided search is performed within this space
 184 to identify the sequence with the highest pre-
 185 dicted performance. The optimized sequence is
 186 then propagated back to clients, where it will be
 187 fused with complementary, non-overlapping lo-
 188 cal transformation sequences to improve client-
 189 specific predictive performance.
 190

191 4.1.1 AUTOMATED LOCAL FEATURE TRANSFORMATION RECORDS COLLECTION.

192 To learn a unified and generalizable feature transformation representation, it is essential to thor-
 193oughly explore the intrinsic characteristics of tabular data within each client. We apply a rein-
 194forcement learning (RL) framework Wang et al. (2022; 2023) on each client’s \mathcal{D} to efficiently collect
 195 transformation sequence–model performance pairs $\mathcal{R} = \{\Upsilon, v\}$. Specifically, each client employs
 196 a simple three-agent RL framework to collect transformation records. Two agents select candidate
 197 features, and a third selects a mathematical operation from a predefined set. The selected features
 198 are crossed using the chosen operation to generate a new feature, which is added back to the feature
 199 set for further refinement. This process iteratively explores transformation sequences that maximize
 200 downstream task performance. *Importantly, the local collector is modular: clients with different re-*
 201 *source budgets can plug in non-RL alternatives, and the server aggregates their records in a method-*
 202 *agnostic manner.* The collected transformation sequences and associated model performance scores
 203 are subsequently uploaded to the central server for aggregation. As no raw data is exchanged during
 204 this process, the framework inherently preserves data privacy and mitigates potential exposure risks.
 205

206 4.1.2 ENCODER-DECODER-EVALUATOR GLOBAL KNOWLEDGE AGGREGATION.

207 To derive a unified and generalizable feature transformation sequence, it is essential to aggregate
 208 transformation knowledge from diverse clients for further refinement. To this end, we propose an
 209 encoder–decoder–evaluator architecture that embeds the collected transformation records from all
 210 clients into a shared cross-client embedding space. The objective is to construct a latent space in
 211 which each embedding point corresponds to a transformation sequence Υ and its associated pre-
 212 dicted model performance v , enabling the capture of transferable transformation patterns across
 213 heterogeneous tabular data. The model is jointly trained with three objectives: a reconstruction loss
 214 ensuring accurate sequence recovery, a performance estimation loss for reliable performance predic-
 215 tion, and a KL regularization term promoting smoothness in the embedding space landscape. This
 joint objective aligns the embedding space with both the structural and semantic characteristics of
 transformation sequences, supporting effective global optimization in downstream tasks.

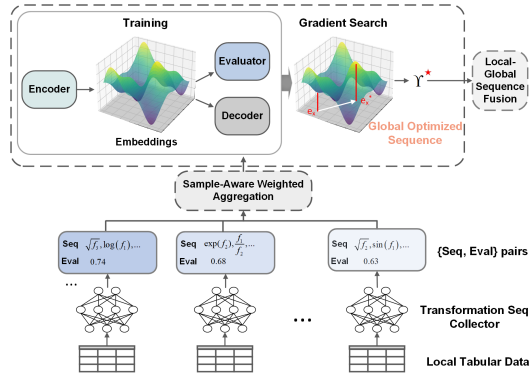


Figure 1: Framework overview of FEDFT. Clients generate transformation records locally and upload them with sample metrics. The server aggregates, learns embeddings, and returns the optimal sequence for local refinement.

216 *Encoder ϕ :* The encoder component effectively maps a given transformation sequence Υ into a
 217 continuous embedding vector \mathbf{E} . We utilize a single-layer Long Short-Term Memory (LSTM) net-
 218 work Hochreiter & Schmidhuber (1997), where the resulting output is denoted as $\mathbf{E} = \phi(\Upsilon) \in$
 219 $\mathbb{R}^{M \times d}$, with M being the input sequence length and d the embedding hidden dimension.

220 *Decoder ψ :* The decoder component reconstructs the original transformation sequence from the en-
 221 coder embedding. Implemented as a single-layer LSTM, the decoder takes an initial state h_0 and
 222 updates its hidden state h_i^d at each step. We apply dot-product attention between the decoder hidden
 223 state h_i^d and the encoder outputs to produce a context vector h_i^e . The token distribution at step i is
 224

225
$$P_\psi(\gamma_i \mid \mathbf{E}, \Upsilon_{<i}) = \frac{\exp(W_{\gamma_i}(h_i^d \oplus h_i^e))}{\sum_{c \in \mathcal{C}} \exp(W_c(h_i^d \oplus h_i^e))},$$
 where \mathcal{C} is the token vocabulary, and \oplus denotes concate-
 226 nation. The probability of generating the full sequence is: $P_\psi(\Upsilon \mid \mathbf{E}) = \prod_{i=1}^M P_\psi(\gamma_i \mid \mathbf{E}, \Upsilon_{<i}),$
 227 which captures the step-wise generation process. We train by minimizing the reconstruction loss
 228 $\mathcal{L}_{\text{rec}} = -\log P_\psi(\Upsilon \mid \mathbf{E})$, which encourages assigning high probability to the true sequence.
 229

230 *Evaluator ω :* The evaluator component estimates the model performance v from the embedding \mathbf{E} .
 231 We first perform mean pooling operation to obtain a fixed-length vector $\bar{\mathbf{E}} \in \mathbb{R}^d$, which is then
 232 passed through a multi-layer feedforward network: $\hat{v} = \omega(\bar{\mathbf{E}})$. The estimation loss is computed as
 233 the mean squared error between predicted and real accuracy: $\mathcal{L}_{\text{est}} = \text{MSE}(v, \omega(\bar{\mathbf{E}}))$. To encourage
 234 a smooth latent embedding space for the inference stage, we further map $\bar{\mathbf{E}}$ to the mean and log-
 235 variance of a Gaussian with MLP layers, obtaining vectors $\mu, \log \sigma^2$. We then construct a KL
 236 regularizer with standard reparameterization tricks: $\mathcal{L}_{\text{KL}} = \frac{1}{2} \sum_{j=1}^d (\mu_j^2 + \sigma_j^2 - 1 - \log \sigma_j^2)$.
 237

238 *Joint Training Loss \mathcal{L} :* The encoder, decoder, and evaluator are jointly trained with a weighted loss:
 239
$$\mathcal{L} = (1 - \lambda)\mathcal{L}_{\text{rec}} + \lambda\mathcal{L}_{\text{est}} + \beta\mathcal{L}_{\text{KL}}$$
, where λ balances predictive performance estimation and β
 240 regularizes the embedding space to enhance smoothness for exploration. During training, the se-
 241 quence–performance pairs are embedded into a latent space that is jointly optimized for smoothness
 242 and predictive accuracy. Smoothness ensures geometric continuity for effective exploration, while
 243 the evaluation loss provides explicit performance guidance. This dual regularization reduces the
 244 impact of data heterogeneity and encourages the learning of robust, generalizable representations.
 245

246 *Gradient-based Optimal sequence Search:* After training, we select the top- T candidate transforma-
 247 tion sequences ranked by their average predictive performance \bar{v} across clients. These are encoded
 248 into continuous embeddings using the trained encoder, serving as seeds for gradient search. Let \mathbf{E}
 249 denote one such embedding. We update \mathbf{E} by ascending along the gradient provided by evaluator
 250 ω , following $\tilde{\mathbf{E}} = \mathbf{E} + \eta \frac{\partial \omega}{\partial \mathbf{E}}$, where η is the size of search step. This update is expected to improve
 251 predicted performance, i.e., $\omega(\tilde{\mathbf{E}}) > \omega(\mathbf{E})$. We then decode $\tilde{\mathbf{E}}$ back to a transformation sequence
 252 and select the one with the highest average predictive performance as the globally optimal sequence.
 253

4.2 SAMPLE-AWARE WEIGHTED AGGREGATION FOR OPTIMIZATION BIAS CORRECTION

254 **Why Sample-Aware Scheme on Global Knowledge Aggregation.** After collecting the transforma-
 255 tion–performance records from different clients, we observe that the reliability of these records
 256 varies significantly due to heterogeneous local tabular data characteristics. Specifically, varying
 257 sample sizes, feature diversity, and numerical stability. This multifaceted heterogeneity is partic-
 258 ularly pronounced in tabular settings due to inherent sparsity and heterogeneous feature types. It
 259 fundamentally reflects differences in the information content and reliability of local performance
 260 signals. Clients with limited data tend to provide less informative and noisier signals, while those with
 261 larger, diverse, stable datasets offer more reliable performance indicators. Consequently, directly
 262 incorporating these unadjusted scores into the server-side encoder–decoder–evaluator architecture
 263 can introduce bias and compromise global model generalizability. To address this, we introduce a
 264 sample-aware weighted aggregation strategy, where each client’s contribution is scaled by its dataset
 265 size, diversity, and stability indicators. This approach enhances statistical stability, reduces the im-
 266 pact of unreliable signals, and supports the learning of a more generalizable embedding space.
 267

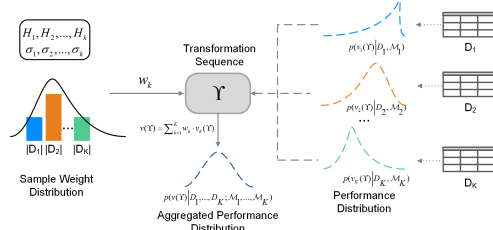
268 As illustrated in Figure 2, even for the same transformation sequence and a fixed down-
 269 stream model family, the observed performance scores across clients follow distinct distribu-
 270 tions. As mentioned earlier, using these unadjusted scores directly would bias the server
 271 model and reduce its generalizability. To mitigate this issue and obtain a more reliable
 272 model performance estimation, we implement a sample-aware weighted aggregation strategy

270 that corrects for distributional bias. Specifically, we first collect all transformation records
 271 from local clients and construct a non-redundant set of transformation sequences on the server.
 272 Each sequence is then broadcast to all K clients, who apply the transformation to their local tabu-
 273 lar data and evaluate the resulting model performance. As a result, each transformation sequence
 274 is associated with a set of K client-specific performance scores, denoted as $[\hat{v}_1, \hat{v}_2, \dots, \hat{v}_K]$. We
 275 compute client weights by combining two complementary factors—dataset size and data quality—
 276 with the overall weight formulated as $w_k = p \cdot w_k^{(size)} + (1 - p) \cdot w_k^{(adj)}$. The size-based term
 277 $w_k^{(size)} = \frac{|D_k|}{\sum_{j=1}^K |D_j|}$ captures the relative sample
 278 proportion, and the quality-based term $w_k^{(adj)} = \frac{s_k}{\sum_{j=1}^K s_j}$, where $s_k = q \cdot H_k + (1 - q) \cdot \sigma_k$ in-
 279 corporates feature entropy H_k (diversity) and stability score σ_k (derived from condition number κ_k).
 280 Here, higher feature entropy indicates more diverse information content, while lower condition num-
 281 bers (higher stability scores) suggest better numerical stability and reduced multicollinearity risk.
 282 This weighting scheme reflects that performance estimates from larger datasets are more reliable,
 283 while diverse feature information and numerical stability enhance local signal quality. The final
 284 aggregated score for a transformation sequence Υ is computed as: $v = \sum_{k=1}^K w_k \cdot \hat{v}_k$.

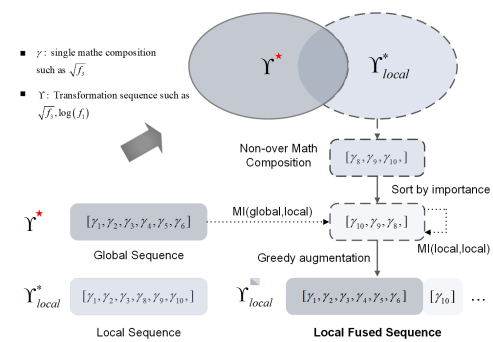
293 4.3 GLOBAL-TO-LOCAL FEATURE INTEGRATION UNDER MUTUAL INFORMATION CONTROL

294 **Why Dual Optimization for Local and Global Perspectives Is Essential.** After federated
 295 aggregation and server-side optimization, we obtain a globally optimized feature transformation se-
 296 quence that captures domain-level knowledge across
 297 diverse clients. This sequence can serve as a foun-
 298 dation for further domain understanding and analy-
 299 sis. However, clients are typically more concerned
 300 with improving performance on their own local pre-
 301 dictive tasks rather than contributing to global un-
 302 derstanding. Relying solely on local data and pat-
 303 terns may lead to overfitting and hinder generaliza-
 304 tion, while indiscriminately aggregating local contri-
 305 butions may fail to satisfy individual clients’ objec-
 306 tives, threatening the sustainability of collaboration.
 307 To address this issue, we adopt a dual-benefit strat-
 308 egy: the globally optimized transformation sequence
 309 is fed back to each client, enabling local model re-
 310 finement while preserving the value of global knowl-
 311 edge. This not only incentivizes client participation but
 312 also ensures that the collaboration remains
 313 mutually beneficial. By integrating globally informed
 314 transformations, clients can enhance their
 315 models in a way that balances domain-level generalization with client-specific adaptability.

316 As shown in Figure 3, after completing gradient-based search, the server broadcasts the global trans-
 317 formation sequence Υ^* to all clients. To integrate domain-level knowledge with local adaptation,
 318 each client augments Υ^* with a small set of locally distinctive features. Each client begins by select-
 319 ing its local best transformation sequence and extracts derived features as candidates. For each can-
 320 didate, two criteria are computed: (1) a model-dependent feature importance score for initial rank-
 321 ing, and (2) its redundancy with the global features and the currently selected local ones, measured
 322 by mutual information (MI). Let \mathcal{G} denote global features and \mathcal{C} the pool of candidate local features.
 323 The client incrementally builds a supplement set \mathcal{F} by greedily selecting the least redundant feature
 $f \in \mathcal{C}$ at each step, according to the following score: $\text{Score}(f) = \eta \cdot \text{AvgMI}(f, \mathcal{F}) + \delta \cdot \text{AvgMI}(f, \mathcal{G})$,
 where $\text{AvgMI}(f, \cdot)$ denotes the average mutual information between f and the features in the cor-
 responding set. The process continues until a fixed budget is reached or no candidates remain.



295 Figure 2: Sample-Aware weighted
 296 aggregation. Sample characteristics and local
 297 performance distributions are aggregated for
 298 more reliable sequence evaluation.



299 Figure 3: Local-Global sequence fusion.
 300 Local feature space is refined by fusing with
 301 the global sequence

324 Finally, the client builds its personalized feature set by combining global and selected local features:
 325 $\mathcal{Z}_k = \mathcal{G} \cup \mathcal{F}$, where \mathcal{Z}_k is the final augmented feature set used by client k for downstream pre-
 326 dictive modeling. This fused representation preserves domain-level knowledge while incorporating
 327 client-specific insights, yielding consistent improvements under heterogeneous tabular distributions.
 328

329 5 EXPERIMENT

330 5.1 EXPERIMENT SETTINGS

331 **Dataset and Evaluation Metrics.** We use 13 publicly available datasets from UCI Kelly et al.
 332 (2023), LibSVM Lin (2022), and OpenML Public (2022) to conduct our experiments. Table 4 shows
 333 the statistics of the data. Regression tasks were evaluated using the following metrics: 1-Relative
 334 Absolute Error (1-RAE), 1-Mean Absolute Error (1-MAE), 1-Root Mean Squared Error (1-RMSE)
 335 and coefficient of determination (R^2). For classification tasks, assessment was conducted using
 336 Precision, Recall, F1-score and AUC-score. The formulae for the F1-score and 1-RAE are given
 337 by: $F1 = 2 \cdot \frac{\text{Precision} \cdot \text{Recall}}{\text{Precision} + \text{Recall}}$ and $1\text{-RAE} = 1 - \frac{\sum_{i=1}^n |y_i - \bar{y}_i|}{\sum_{i=1}^n |y_i - \bar{y}_i|}$, where y_i , \bar{y}_i , and \bar{y}_i represent the ground
 338 truth, predictions, and the mean of the ground truth, respectively.
 339

340 **Baseline Methods.** To sufficiently evaluate FEDFT, we consider three baseline methods. First, we
 341 compare three transformation sequences: Υ_I , an ideal upper bound obtained by directly optimizing
 342 on global data; Υ^* , the global sequence generated by FEDFT through federated aggregation; and
 343 Υ_{local} , the best locally generated sequence on each client. These are evaluated on both a global test
 344 set and local client test sets to examine generalization and client-level effectiveness. Second, we in-
 345 tegrate FEDFT into standard federated learning frameworks such as FedAvg by allowing each client
 346 to maintain its own transformation module, enabling fair comparison with traditional model-weight
 347 averaging strategies. Third, we conduct ablation studies to isolate the impact of two key com-
 348 ponents: FEDFT^{-u} removes the encoder-decoder-evaluator structure, and FEDFT^{-c} removes the
 349 sample-aware weighted aggregation. These comparisons collectively show the contribution of global
 350 optimization, local adaptation, and aggregation correction to the overall performance of FEDFT.
 351

352 5.2 PERFORMANCE EVALUATION

353 **Overall Performance.** This experiment aims to answer the following questions: *Can our FEDFT*
 354 *framework effectively capture the domain knowledge of an inaccessible global distribution and en-*
 355 *hance local models through globally coordinated feature transformations?* Table 1 shows results
 356 in terms of F1 and 1-RAE. **Global** column reports performance on the unseen global dataset for
 357 reference, while **Local** column shows the average test performance across clients. We report three
 358 variants: Υ_I : the upper bound achieved by gradient search with direct access to global data; Υ^* :
 359 the best sequence selected without global data, based on weighted local performances; Υ_{local} : the
 360 best locally generated feature transformation sequences of each client for average performance. We
 361 observe that FEDFT consistently produces transformation sequences that outperform locally gener-
 362 ated ones in both global and local evaluations. The underlying driver is the complementary effect of
 363 global knowledge aggregation and local feature fusion. For global performance, FEDFT aggregates
 364 information from all clients, capturing the shared structure of the global data distribution. For local
 365 performance, the feature fusion mechanism enriches the local feature space by combining global
 366 knowledge with client-specific features, improving local model effectiveness. In summary, FEDFT
 367 effectively captures global distribution information while refining global and local feature spaces.
 368

369 **Comparison with Federated Baselines.** This experiment aims to answer the following questions:
 370 *Can our FEDFT framework match or outperform the well acknowledged federated learning meth-
 371 ods?* To answer this question, we compare FEDFT with recent feature-transformation-focused
 372 FL method Fed-IIFE Overman & Klabjan (2024) and with established federated learning base-
 373 lines(FedAvg McMahan et al. (2017), FedProx Li et al. (2020), MOON Li et al. (2021) and Fed-
 374 NTD Lee et al. (2022)) that follow a different aggregation strategy: while FEDFT shares feature
 375 transformation-performance pairs, traditional methods rely on model weight aggregation, requir-
 376 ing all clients to adopt the same model structure as the global model. These methods also incur
 377 extra costs, as they maintain both the FEDFT transformation pipeline and a local encoder-decoder-
 378 evaluator module. As shown in Table 2, we conduct experiments on three datasets: Openml_586,
 379 Wine Quality Red, and Pima Indian datasets, using 1-RAE for regression and F1 score for classifi-
 380 cation tasks. For each method, we apply the best feature transformation sequence to both global and
 381 local partitions, reporting mean and standard deviation across all clients for the latter. We observe
 382

378 Table 1: Overall performance comparison. Global and Local columns report results on the global
 379 and local test sets for three sequence variants: Υ_I (ideal upper bound with global data access), Υ^*
 380 (optimal sequence via sample-aware aggregation), and Υ_{local} (client-wise best local sequences).

Dataset	Global			Local	
	Υ_I	Υ^*	Υ_{local}	Υ^*	Υ_{local}
SpectF	0.8234	0.8164	0.7740 ± 0.0210	0.8817	0.8742 ± 0.0050
Pima Indian	0.7725	0.7669	0.7455 ± 0.0083	0.7532	0.7316 ± 0.0042
SVMGuide3	0.8473	0.8473	0.8415 ± 0.0176	0.8439	0.8249 ± 0.0015
Wine Red	0.6843	0.6843	0.6671 ± 0.0061	0.6330	0.6283 ± 0.0089
Wine White	0.6776	0.6760	0.6729 ± 0.0028	0.6646	0.6570 ± 0.0026
Housing Boston	0.6487	0.6487	0.6431 ± 0.0039	0.5826	0.5642 ± 0.0042
Airfoil	0.7892	0.7892	0.7760 ± 0.0060	0.7674	0.7529 ± 0.0022
Openml_620	0.7168	0.7168	0.7030 ± 0.0070	0.6036	0.5935 ± 0.0011
Openml_589	0.7421	0.7409	0.7018 ± 0.0407	0.6238	0.5627 ± 0.0571
Openml_586	0.7742	0.7742	0.6727 ± 0.0076	0.6511	0.5198 ± 0.0119
Openml_637	0.5702	0.5667	0.5575 ± 0.0089	0.3334	0.2884 ± 0.0370
Openml_618	0.7457	0.7457	0.7392 ± 0.0103	0.5959	0.5819 ± 0.0256
Openml_607	0.7395	0.7395	0.6405 ± 0.0117	0.5182	0.4367 ± 0.0218

\pm indicates standard deviation across clients.

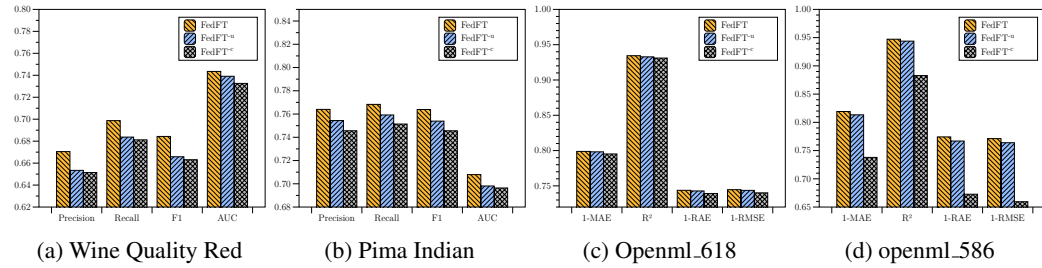


Figure 4: The influence of global aggregation (FedFT^{-c}) and encoder-decoder-evaluator knowledge integration (FedFT^{-u}) in FedFT.

that FEDFT achieves performance comparable to or better than these well-acknowledged models. The underlying reason is that feature transformation sequence-performance pairs carry sufficient information to enable effective aggregation without requiring full model weight sharing. In summary, FEDFT offers an effective and flexible alternative to weight-sharing approaches.

Ablation Study. This experiment aims to answer: *Does the sample-aware weighted aggregation and encoder-decoder-evaluator knowledge internalization help to maintain the performance of FEDFT?* To answer this question, we develop two model variants of FEDFT: 1) FEDFT $^{-u}$, which drops the encoder-decoder-evaluator part, and 2) FEDFT $^{-c}$, which drops the sample-aware weighted aggregation step in FEDFT. We report comparison results in terms of F1 score or 1-RAE on four datasets: Openml_618, Openml_586, Wine Quality Red and Pima Indian. Figure 4 presents the results on global data. We observe that FedFT significantly outperforms FedFT $^{-c}$. This improvement is attributed to the fact that local data silos contain only partial and biased data distributions. Without federated aggregation, models trained on these silos perform poorly when generalized to global data. Second, we find that FedFT consistently achieves better performance than FedFT $^{-u}$. This gain is driven by the encoder-decoder-evaluator module, which not only compresses and smooths the aggregated information but also enables continuous optimization through gradient search, leading to better feature transformation sequences. In summary, both the sample-aware weighted aggregation and the encoder-decoder-evaluator module are essential for preserving the effectiveness of FEDFT and achieving consistent performance improvement over its simplified version.

Impact of KL-Induced Embedding Smoothness on Latent Feature Space Search. This experiment aims to answer: *Whether KL divergence loss enhances the smoothness of the refined latent space and improves the gradient-based search.* To analyze this effect, we visualize the latent space embeddings of two models trained on the Pima Indian dataset: one without KL loss and the other

Table 2: Performance Comparison of Different Federated Learning Algorithms

Method	Openml 586		Wine Red		Pima Indian	
	Global	Local	Global	Local	Global	Local
FedAvg	0.7665	0.6413 \pm 0.0254	0.6706	0.6466 \pm 0.0529	0.7560	0.7513 \pm 0.0414
FedProx	0.6877	0.5051 \pm 0.0433	0.6650	0.6413 \pm 0.0437	0.7457	0.7188 \pm 0.0244
MOON	0.7718	0.6485 \pm 0.0277	0.6675	0.6440 \pm 0.0577	0.7552	0.7528 \pm 0.0623
FedNTD	0.7661	0.6405 \pm 0.0257	0.6765	0.6407 \pm 0.0594	0.7535	0.7556 \pm 0.0492
FedCross	0.7670	0.6413 \pm 0.0254	0.6670	0.6392 \pm 0.0512	0.7540	0.7545 \pm 0.0557
Fed-IIFE	0.7538	0.6106 \pm 0.0186	0.6548	0.6221 \pm 0.1084	0.7478	0.7578 \pm 0.0354
Ours	0.7742	0.6511 \pm 0.0226	0.6843	0.6330 \pm 0.0087	0.7669	0.7532 \pm 0.0418

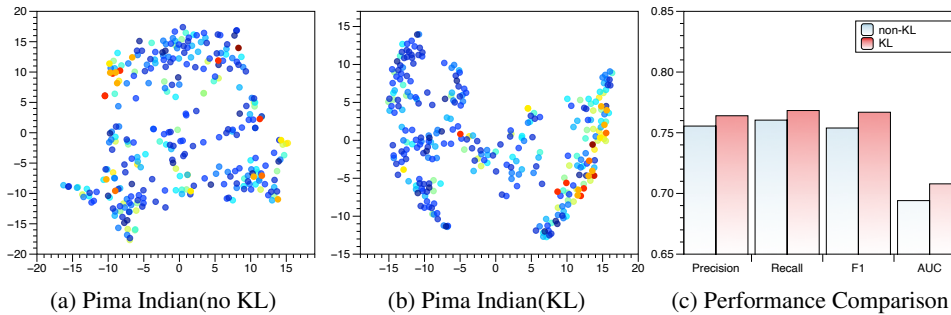


Figure 5: Comparison of latent space smoothness and downstream performance with and without KL loss. (a)-(b) show smoother and more clustered embeddings with KL loss. (c) shows improved downstream performance after gradient search when KL loss is applied.

with KL loss applied in the Figure 5. Warmer-colored points indicate higher performance. We observe that the model trained without KL loss produces a less smooth latent space, where high-performing sequence embeddings are scattered with large performance variations. Conversely, the model trained with KL loss exhibits a smoother latent space, where high-performing sequence embeddings are more tightly clustered with clear, continuous transitions. This indicates that KL loss encourages smoother structuring of the latent space. We further compare the downstream task performance after applying gradient-based search. Results show model with a smoother latent space enables more effective gradient search, finding higher-quality feature transformation sequences. In summary, KL-induced smoothness enhances latent space structure, improving gradient search.

6 CONCLUSION

In this paper, we propose a federated feature transformation framework designed to effectively refine the feature space and aggregate knowledge in tabular data silos settings. The framework centers on two key components: a sample-aware weighted knowledge aggregation module and a local-global sequence fusion scheme. To preserve privacy while enabling knowledge sharing, we introduce a sequence-performance pair communication protocol, allowing clients to share feature transformation knowledge without exposing raw data. To address performance variance and bias from heterogeneous client data, we develop a sample-aware weighted aggregation strategy, which allocates weights to client-reported performance scores based on their local sample characteristics. It ensures that the aggregated evaluation better reflects the overall data distribution and improves server-side training. To dual-optimize both the server and client-side performance, we design a local-global sequence fusion scheme. The server feeds back the globally aggregated transformation sequence, capturing domain-level knowledge, to clients. Each client then fuses this global knowledge with locally distinctive features, improving local predictive tasks while incentivizing client participation. Extensive experiments demonstrate that FEDFT effectively enhances both global and local performance. The proposed sample-aware weighted aggregation mitigates clients' data heterogeneity, while the feedback and fusion scheme benefits individual clients and encourages ongoing contribution and collation across the federation. In future work, we plan to extend FEDFT to dynamic federated environments, where client availability and data distributions evolve over time, and to explore its integration with automated feature generation and task-adaptive personalization strategies.

486 REFERENCES
487

488 Yoshua Bengio, Aaron Courville, and Pascal Vincent. Representation learning: A review and new
489 perspectives. *IEEE transactions on pattern analysis and machine intelligence*, 35(8):1798–1828,
490 2013.

491 Vincent Bindschaedler and Reza Shokri. Synthesizing plausible privacy-preserving location traces.
492 In *2016 IEEE symposium on security and privacy (SP)*, pp. 546–563. IEEE, 2016.

493

494 Keith Bonawitz, Vladimir Ivanov, Ben Kreuter, Antonio Marcedone, H Brendan McMahan, Sarvar
495 Patel, Daniel Ramage, Aaron Segal, and Karn Seth. Practical secure aggregation for privacy-
496 preserving machine learning. In *proceedings of the 2017 ACM SIGSAC Conference on Computer
497 and Communications Security*, pp. 1175–1191, 2017.

498 Pietro Cassarà, Alberto Gotta, and Lorenzo Valerio. Federated feature selection for cyber-physical
499 systems of systems. *IEEE Transactions on Vehicular Technology*, 71(9):9937–9950, 2022.

500

501 Xiangning Chen, Qingwei Lin, Chuan Luo, Xudong Li, Hongyu Zhang, Yong Xu, Yingnong Dang,
502 Kaixin Sui, Xu Zhang, Bo Qiao, et al. Neural feature search: A neural architecture for automated
503 feature engineering. In *2019 IEEE International Conference on Data Mining (ICDM)*, pp. 71–80.
504 IEEE, 2019.

505 Úlfar Erlingsson, Vitaly Feldman, Ilya Mironov, Ananth Raghunathan, Kunal Talwar, and
506 Abhradeep Thakurta. Amplification by shuffling: From local to central differential privacy via
507 anonymity. In *Proceedings of the Thirtieth Annual ACM-SIAM Symposium on Discrete Algo-
508 rithms*, pp. 2468–2479. SIAM, 2019.

509

510 Pei Fang, Zhendong Cai, Hui Chen, and QingJiang Shi. Flfe: a communication-efficient and privacy-
511 preserving federated feature engineering framework. *arXiv preprint arXiv:2009.02557*, 2020.

512 Rui Fu, Yuncheng Wu, Quanqing Xu, and Meihui Zhang. Feast: A communication-efficient feder-
513 ated feature selection framework for relational data. *Proceedings of the ACM on Management of
514 Data*, 1(1):1–28, 2023.

515

516 Huifeng Guo, Ruiming Tang, Yunming Ye, Zhenguo Li, and Xiuqiang He. Deepfm: a factorization-
517 machine based neural network for ctr prediction. *arXiv preprint arXiv:1703.04247*, 2017.

518

519 Sepp Hochreiter and Jürgen Schmidhuber. Long short-term memory. *Neural computation*, 9(8):
520 1735–1780, 1997.

521

522 Franziska Horn, Robert Pack, and Michael Rieger. The autofeat python library for automated feature
523 engineering and selection. In *Joint European Conference on Machine Learning and Knowledge
524 Discovery in Databases*, pp. 111–120. Springer, 2019.

525

526 James Max Kanter and Kalyan Veeramachaneni. Deep feature synthesis: Towards automating data
527 science endeavors. In *2015 IEEE international conference on data science and advanced analyt-
ics (DSAA)*, pp. 1–10. IEEE, 2015.

528

529 Sai Praneeth Karimireddy, Satyen Kale, Mehryar Mohri, Sashank Reddi, Sebastian Stich, and
530 Ananda Theertha Suresh. Scaffold: Stochastic controlled averaging for federated learning. In
531 *International conference on machine learning*, pp. 5132–5143. PMLR, 2020.

532

533 Markelle Kelly, Rachel Longjohn, and Kolby Nottingham. The uci machine learning repository,
2023.

534

535 Udayan Khurana, Deepak Turaga, Horst Samulowitz, and Srinivasan Parthasarathy. Cognito: Auto-
536 mated feature engineering for supervised learning. In *2016 IEEE 16th international conference
537 on data mining workshops (ICDMW)*, pp. 1304–1307. IEEE, 2016.

538

539 Udayan Khurana, Horst Samulowitz, and Deepak Turaga. Feature engineering for predictive mod-
eling using reinforcement learning. In *Proceedings of the AAAI Conference on Artificial Intelli-
gence*, volume 32, 2018.

540 Gihun Lee, Minchan Jeong, Yongjin Shin, Sangmin Bae, and Se-Young Yun. Preservation of the
 541 global knowledge by not-true distillation in federated learning. *Advances in Neural Information*
 542 *Processing Systems*, 35:38461–38474, 2022.

543

544 Qinbin Li, Bingsheng He, and Dawn Song. Model-contrastive federated learning. In *Proceedings of*
 545 *the IEEE/CVF conference on computer vision and pattern recognition*, pp. 10713–10722, 2021.

546

547 Tian Li, Anit Kumar Sahu, Manzil Zaheer, Maziar Sanjabi, Ameet Talwalkar, and Virginia Smith.
 548 Federated optimization in heterogeneous networks. *Proceedings of Machine learning and sys-*
 549 *tems*, 2:429–450, 2020.

550

551 Chih-Jen Lin. Libsvm dataset download [eb/ol]. <https://www.csie.ntu.edu.tw/~cjlin/libsvm/>, 2022.

552

553

554 Brendan McMahan, Eider Moore, Daniel Ramage, Seth Hampson, and Blaise Aguera y Arcas.
 555 Communication-efficient learning of deep networks from decentralized data. In *Artificial intelli-*
 556 *gence and statistics*, pp. 1273–1282. PMLR, 2017.

557

558 Tom Overman and Diego Klabjan. Federated automated feature engineering. *arXiv preprint*
 559 *arXiv:2412.04404*, 2024.

560

561 Public. Openml dataset download [eb/ol]. <https://www.openml.org>, 2022.

562

563 Mohammad Rasouli, Tao Sun, and Ram Rajagopal. Fedgan: Federated generative adversarial net-
 564 works for distributed data. *arXiv preprint arXiv:2006.07228*, 2020.

565

566 MyungJae Shin, Chihoon Hwang, Joongheon Kim, Jihong Park, Mehdi Bennis, and Seong-Lyun
 567 Kim. Xor mixup: Privacy-preserving data augmentation for one-shot federated learning. *arXiv*
 568 *preprint arXiv:2006.05148*, 2020.

569

570 Binh Tran, Bing Xue, and Mengjie Zhang. Genetic programming for feature construction and se-
 571 lection in classification on high-dimensional data. *Memetic Computing*, 8:3–15, 2016.

572

573 Dongjie Wang, Yanjie Fu, Kunpeng Liu, Xiaolin Li, and Yan Solihin. Group-wise reinforcement fea-
 574 ture generation for optimal and explainable representation space reconstruction. In *Proceedings of*
 575 *the 28th ACM SIGKDD Conference on Knowledge Discovery and Data Mining*, pp. 1826–1834,
 576 2022.

577

578 Dongjie Wang, Meng Xiao, Min Wu, Yuanchun Zhou, Yanjie Fu, et al. Reinforcement-enhanced
 579 autoregressive feature transformation: Gradient-steered search in continuous space for postfix
 580 expressions. *Advances in Neural Information Processing Systems*, 36:43563–43578, 2023.

581

582 Tehrim Yoon, Sumin Shin, Sung Ju Hwang, and Eunho Yang. Fedmix: Approximation of mixup
 583 under mean augmented federated learning. *arXiv preprint arXiv:2107.00233*, 2021.

584

585 Jianqing Zhang, Yang Liu, Yang Hua, Hao Wang, Tao Song, Zhengui Xue, Ruhui Ma, and Jian
 586 Cao. Pfllib: A beginner-friendly and comprehensive personalized federated learning library and
 587 benchmark. *Journal of Machine Learning Research*, 26(50):1–10, 2025.

588

589 Xunzheng Zhang, Alex Mavromatis, Antonis Vafeas, Reza Nejabati, and Dimitra Simeonidou. Fed-
 590 erated feature selection for horizontal federated learning in iot networks. *IEEE Internet of Things*
 591 *Journal*, 10(11):10095–10112, 2023.

592

593 Guanghui Zhu, Zhuoer Xu, Chunfeng Yuan, and Yihua Huang. Difer: differentiable automated
 594 feature engineering. In *International Conference on Automated Machine Learning*, pp. 17–1.
 595 PMLR, 2022.

594 **A APPENDIX**595 **A.1 EXPERIMENTAL SETTINGS AND REPRODUCIBILITY**596 **A.1.1 EXPERIMENTAL PLATFORM INFORMATION**

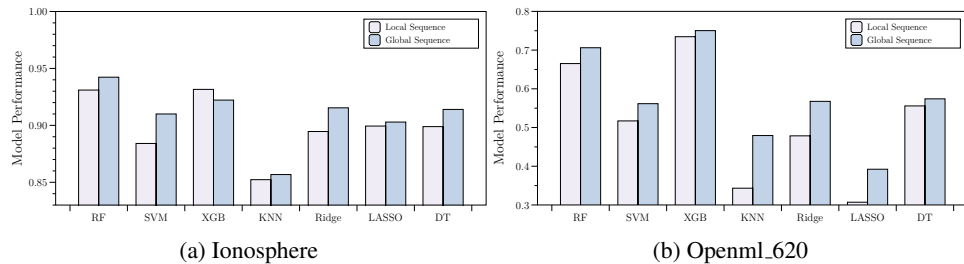
600 All experiments are conducted on an Ubuntu 22.04.5 LTS operating system, powered by an AMD
 601 Ryzen Threadripper PRO 7965WX 24-core processor, equipped with two NVIDIA RTX A6000
 602 GPUs (48GB memory each). Python 3.12.7 and PyTorch 2.5.1 are used as the software framework.
 603

604 **A.1.2 HYPERPARAMETER SETTINGS AND REPRODUCIBILITY**

605 The operation set includes square root, square, cosine, sine, tangent, exponential, cube, logarithm,
 606 reciprocal, quantile transformer, min-max scaler, sigmoid, addition, subtraction, multiplication, and
 607 division. For data collection, we ran the RL-based data collector on each local client’s data for 512
 608 epochs with 10 steps per epoch, gathering a large number of feature transformation–accuracy pairs.
 609 For data augmentation, we randomly shuffled each transformation sequence 12 times to increase
 610 data diversity and volume, applying a token mask probability of 0.3 and a disorder probability of
 611 0.1. We adopted a single-layer LSTM as both the encoder and decoder backbones, and a three-layer
 612 feed-forward network as the predictor. The hidden sizes of the encoder, decoder, and predictor were
 613 set to 64, 64, and 200, respectively. The embedding size for both feature ID tokens and operation
 614 tokens was set to 32. FedFT was trained with a batch size of 32, a learning rate of 0.001, $\lambda = 0.95$,
 615 and $\beta = 0.001$. For inference, we used the top-50 records as seed sequences. For data segmentation,
 616 regression datasets were partitioned into equal blocks without random disturbance to preserve
 617 segmentation differences. For classification datasets, we used an α ranging from 0.5 to 1.0 to divide
 618 the data based on the number of samples in each dataset. For the aggregation mechanism, we allo-
 619 cate 90% weight to performance metrics and 10% to feature diversity and stability considerations.
 620 For the baseline experiments presented in Table 2, we adapted our model based on the framework
 621 introduced by Zhang et al. Zhang et al. (2025).
 622

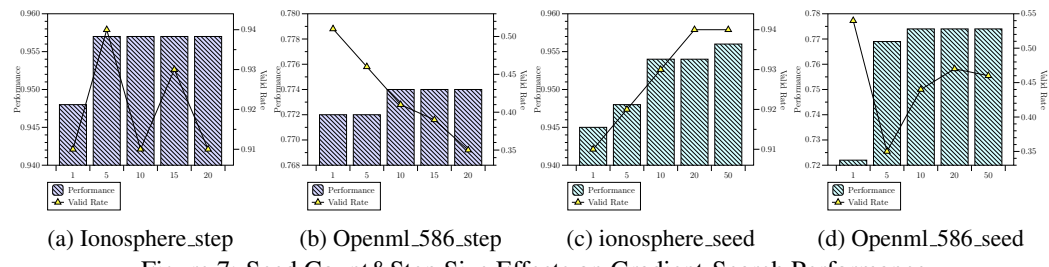
623 **A.2 EXPERIMENTAL RESULTS**624 **A.2.1 ROBUSTNESS CHECK**

626 This experiment aims to answer: *Does FedFT exhibit robustness when confronted with various ma-*
 627 *chine learning models serving as downstream tasks?* To investigate, we replace the downstream ma-
 628 *chine learning model with Random Forest (RF), Support Vector Machine (SVM), XGBoost (XGB),*
 629 *K-Nearest Neighbors (KNN), Ridge Regression (Ridge), LASSO Regression (LASSO), and De-*
 630 *cision Tree (DT), respectively. Figure 6 presents the comparison results in terms of F1 and 1-RAE on*
 631 *the Ionosphere and Openml_620 datasets. We observe that, regardless of the choice of downstream*
 632 *models, FedFT consistently facilitates the construction of more generalized feature transformation*
 633 *sequences at a global scale, compared to locally derived sequences. This effect can be attributed to*
 634 *the fact that when local samples are limited or biased, FedFT aggregates information from mul-*
 635 *tiple clients to capture domain knowledge that reflects the global feature space—knowledge that is*
 636 *otherwise inaccessible to individual clients. Thus, this experiment demonstrates the robustness of*
 637 *FedFT in refining feature space across different downstream machine learning models.*

647 **Figure 6: Robustness Check of FedFT when confronted with different downstream ML models**

648 A.2.2 IMPACT OF SEED AND STEP HYPERPARAMETERS ON VALIDATION STABILITY AND 649 GRADIENT SEARCH PERFORMANCE 650

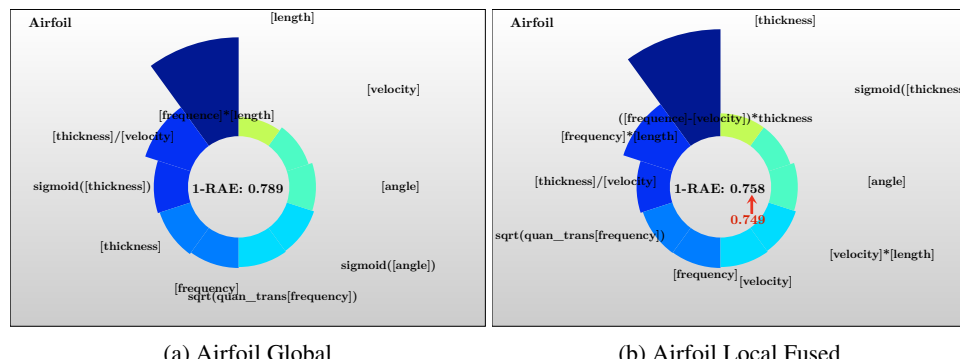
651 This experiment aims to answer: *How do the seed number and search step size affect the gradient-
652 guided sequence optimization process?* To address this question, we conduct experiments by
653 varying the gradient search step size and the number of top seeds used for optimization. Specifically,
654 we perform evaluations on the Ionosphere and OpenML_586 datasets. For the search step size, we
655 test values ranging from 1 to 20, and for the number of seeds, we evaluate settings from 1 to 50.
656 As shown in figure 7. Our observations show that increasing both the number of seeds and the
657 search step size expands the search space, leading to improved performance. However, regarding
658 the validation rate of newly generated sequences, we find that as the search step increases, the
659 validation rate tends to decline due to greater deviation from the original seed embeddings. Notably,
660 when the initial validation rate is relatively high, this performance drop is less severe.
661



662 Figure 7: Seed Count&Step Size Effects on Gradient-Search Performance

663 A.2.3 CASE STUDY

664 We selected the top 10 essential features for prediction from both the globally optimized sequence
665 and a fused sequence on a subset of the Airfoil dataset. We evaluate the traceability and the effect
666 of global-local feature fusion. In Airfoil Global, the chart shows the globally optimized features
667 result, while Airfoil Local presents the fused sequence combining globally optimized features with
668 additional locally critical, non-redundant features. As shown in Figure 8, we observe that the
669 feature spaces differ between global and local data distributions, with some features being uniquely
670 important for specific clients, reflecting data heterogeneity. The fusion operation helps improve lo-
671 cal model performance by retaining locally relevant features. The top-ranked features capture key
672 physical interactions: frequency directly relates to acoustic emissions, while combinations such as
673 thickness divided by velocity and frequency multiplied by length reflect how airfoil geometry and
674 flow dynamics jointly influence sound generation. Furthermore, nonlinear transformations, such as
675 sigmoid(thickness), enhance feature expressiveness, enabling domain experts to trace the underlying
676 physical factors and derive interpretable analysis rules for evaluating system performance.
677



678 Figure 8: Case study on Airfoil dataset: Global and Local-Fusion

679 A.2.4 PERFORMANCE ANALYSIS UNDER VARYING DATA HETEROGENEITY CONDITIONS

680 This experiment aims to answer the answer: *Does FEDFT maintain robustness and provide consis-
681 tent benefits under varying levels of data heterogeneity across data silos?* To investigate this, we
682 evaluate FEDFT, on three datasets (Wine Red, Spectf, and SVMGuide3) under three distinct data
683

702
703
704
705
706
707
708
709
710
711
712
713
714
715
716
717
718
719
720
721
722
723
724
725
726
727
728
729
730
731
732
733
734
735
736
737
738
739
740
741
742
743
744
745
746
747
748
749
750
751
752
753
754
755

Table 3: Performance of FEDFT under different heterogeneity levels. We report global sequence performance and local best sequence performance (mean \pm std) across three datasets.

Dataset	Method	Heterogeneity Level		
		Centralized	Dir($\alpha=1.0$)	Dir($\alpha=0.5$)
Wine Red	Global (FEDFT)	0.686	0.6730	0.6843
	Global (Local)	-	0.6661 \pm 0.0062	0.6671 \pm 0.0061
	Local (FEDFT)	-	0.6519	0.6330
	Local (Local)	-	0.6379 \pm 0.0077	0.6283 \pm 0.0089
Spectf	Global (FEDFT)	0.878	0.7802	0.8164
	Global (Local)	-	0.7740 \pm 0.0210	0.7740 \pm 0.0210
	Local (FEDFT)	-	0.8174	0.8817
	Local (Local)	-	0.7972 \pm 0.0013	0.8742 \pm 0.0050
SVMGuide3	Global (FEDFT)	0.850	0.8379	0.8473
	Global (Local)	-	0.8310 \pm 0.0025	0.8415 \pm 0.0176
	Local (FEDFT)	-	0.8225	0.8439
	Local (Local)	-	0.8044 \pm 0.0047	0.8249 \pm 0.0015

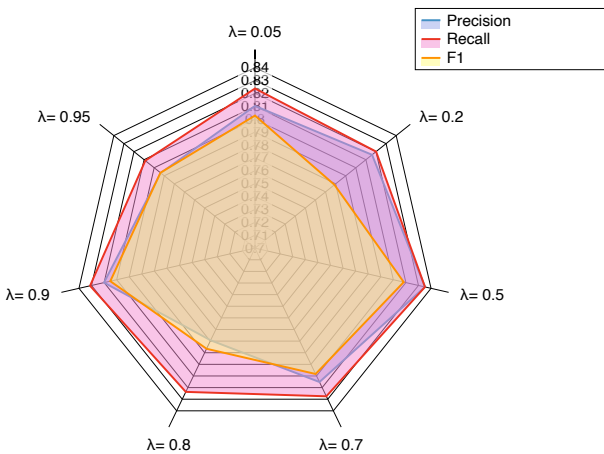
heterogeneity settings: 1) Centralized setting: All data is pooled together (baseline); 2) Moderate heterogeneity: Dirichlet distribution with $\alpha = 1.0$; 3) High heterogeneity: Dirichlet distribution with $\alpha = 0.5$. We report F1 scores as the evaluation metric for transformation sequences generated by FEDFT, and compare them with each local client’s best sequences. These metrics are evaluated on both global and local test datasets to comprehensively investigate the benefits and robustness of FEDFT, with mean and standard deviation reported across clients for later. We observe that FEDFT consistently refines both global and local feature spaces across different heterogeneity levels. Specifically, for Wine Red and SVMGuide3 datasets, the federated learning performance closely approximates the centralized training baseline, indicating strong robustness to data heterogeneity. For the Spectf dataset, while FEDFT improves performance compared to individual client baselines, a notable performance gap remains relative to the centralized setting. The underlying driver of these results is that FEDFT effectively aggregates knowledge across distributed clients, enabling performance improvements in federated settings. The model successfully captures and shares beneficial transformation patterns across silos. However, extreme cases like Spectf present unique challenges—with only 267 global samples across 44 features partitioned into 3 highly heterogeneous segments. In such scenarios, the severe data scarcity per client significantly distorts local performance signals, limiting the effectiveness of knowledge aggregation. In summary, FEDFT demonstrates robust performance across varying heterogeneity levels and consistently enhances feature space refinement and knowledge aggregation in federated tabular data environments. The model effectively bridges the performance gap between isolated data silos and centralized training, providing substantial benefits even under challenging heterogeneous conditions.

A.3 HYPERPARAMETER SENSITIVITY OF λ

This experiment aims to answer: *Is FEDFT sensitive to the choice of λ during encoder-decoder-evaluator training?* To analyze this, we vary λ while keeping all other architectural and training settings fixed, and report the average precision, recall, and F1 over 5-fold validation. We observe that although the metrics show slight fluctuations across different λ values, they remain within a narrow range, indicating that our encoder-decoder-evaluator architecture is robust to the choice of λ for balancing prediction and reconstruction losses.

A.4 COMMUNICATION COSTS AND SECURE COMPUTATIONS

We propose to construct transformation sequence-performance pairs without directly sharing the raw data, so that raw features and labels remain on the clients and are never transmitted to the server. The original raw data resides in $\mathbb{R}^{n \times d}$, where n is the sample size and d is the feature dimension.

Figure 9: Hyperparameter Sensitivity of λ on Spectf

In contrast, our method only requires transmitting the tokenized sequence of length L and a scalar metric, with a payload size of $\mathbb{R}^{L \times 1}$. We assume $n \gg L$. Consequently, communicating abstract sequences significantly reduces communication costs when n is large enough. Furthermore, in scenarios where each client is strictly required not to share explicit local performance statistics or the source of transformation sequences, our architecture can incorporate Secure Aggregation Bonawitz et al. (2017) and the Shuffle Model Erlingsson et al. (2019). This integration allows the server to collectively compute the global ranking and obtain a pool of transformation sequences without accessing individual performance values or tracing the sequence origin, decoupling the data utility from client identity. Moreover, regarding the server-to-client feedback loop, if local clients are restricted from inferring the attribute values or data distributions of other peers through the broadcasted global sequences, our framework supports a Source Obfuscation strategy via Synthetic Sequence Injection. By strategically injecting server-generated “decoy” sequences into the broadcast pool ($\mathcal{S}_{\text{broadcast}} = \mathcal{S}_{\text{real}} \cup \mathcal{S}_{\text{synthetic}}$), we construct a probabilistic barrier. This mechanism leverages the principle of plausible deniability Bindschaedler & Shokri (2016), preventing malicious clients from confidently distinguishing whether a sequence represents a high-value insight from other peers or synthetic noise. It is worth noting that some secure computation techniques can introduce significant computation overhead. To further enhance privacy protection and computational efficiency, it would be beneficial to further improve our proposed method, and we leave it for future exploration.

A.5 LIMITATIONS

While our current framework employs an LSTM-based sequence encoder, we recognize the potential for further improvements in efficiency and representation capacity through more advanced seq2seq models such as transformers. In future work, we plan to explore transformer-based and other state-of-the-art sequence modeling techniques to enhance computational performance and capture richer feature interaction patterns. Additionally, we aim to further investigate non-IID mitigation strategies tailored to our setting and expand our framework to support broader data types beyond tabular data.

A.6 DATASET STATISTICS

A.7 FEATURE ENTROPY AND CONDITION NUMBER

The feature entropy H measures the diversity of features in the dataset. For each feature j in dataset \mathcal{D} with n features:

$$H_j = \begin{cases} -\sum_{i=1}^{u_j} p_{ij} \log(p_{ij}), & \text{if } u_j \leq 10 \text{ (discrete)} \\ -\sum_{b=1}^B p_{bj} \log(p_{bj}), & \text{if } u_j > 10 \text{ (continuous)} \end{cases} \quad (1)$$

Table 4: Data Statistics. ‘C’ for classification and ‘R’ for regression.

Dataset	Source	C/R	Samples	Features	Partitions
SpectF	UCIrvine	C	267	44	3
PimaIndian	UCIrvine	C	768	8	4
SVMGuide3	LibSVM	C	1243	21	5
Wine Red	UCIrvine	C	999	12	5
Wine White	UCIrvine	C	4900	12	10
Ionosphere	UCIrvine	C	351	34	3
Housing Boston	UCIrvine	R	506	13	5
Airfoil	UCIrvine	R	1503	5	5
Openml_620	OpenML	R	1000	25	4
Openml_589	OpenML	R	1000	25	5
Openml_586	OpenML	R	1000	25	4
Openml_637	OpenML	R	500	50	5
Openml_618	OpenML	R	1000	50	5
Openml_607	OpenML	R	1000	50	5

where u_j is the number of unique values for feature j , p_{ij} is the probability of value i in feature j , B is the number of bins (set to 10), and p_{bj} is the probability mass in bin b . The normalized entropy for each feature is:

$$\hat{H}_j = \frac{H_j}{H_{\max,j}}, \quad \text{where } H_{\max,j} = \begin{cases} \log(u_j), & \text{if discrete} \\ \log(B), & \text{if continuous} \end{cases} \quad (2)$$

The overall feature entropy for the dataset is: $H(\mathcal{D}) = \frac{1}{n} \sum_{j=1}^n \hat{H}_j$. The numerical stability is assessed through the condition number of the standardized correlation matrix. Let $\mathbf{X} \in \mathbb{R}^{m \times n}$ be the standardized feature matrix. The correlation matrix is: $\mathbf{R} = \frac{1}{m-1} \mathbf{X}^T \mathbf{X}$. The condition number κ is computed from the eigenvalues $\{a_1, a_2, \dots, a_n\}$ of \mathbf{R} :

$$\kappa(\mathbf{R}) = \frac{a_{\max}}{a_{\min}}, \quad \text{where } a_i > 10^{-10} \quad (3)$$

The stability score σ_k is then derived using an exponential decay function: $\sigma_k = \exp(-0.1 \cdot (\kappa - 1))$. This score is clipped to $[0, 1]$, where values closer to 1 indicate better numerical stability.

864
865 **Algorithm 1:** Postfix transformation sequence conversion
866 **input:** Feature transformation sequence Γ
867 **output:** Postfix-notation based transformation sequence Υ
868 $\Upsilon \leftarrow \emptyset$;
869 **foreach** $\tau \in \Gamma$ **do**
870 $S_1, S_2 \leftarrow \emptyset, \emptyset$;
871 **foreach** token γ in τ **do**
872 **if** γ is a left bracket **then**
873 $S_1.\text{push}(\gamma)$;
874 **else if** γ is a right bracket **then**
875 **while** ($t \leftarrow S_1.\text{pop}()$) is not a left bracket **do**
876 $S_2.\text{push}(t)$;
877 **else if** γ is an operation **then**
878 **while** $S_1.\text{peek}()$ is not a left bracket **do**
879 $S_2.\text{push}(S_1.\text{pop}())$;
880 $S_1.\text{push}(\gamma)$;
881 **else**
882 $S_2.\text{push}(\gamma)$;
883 **while** $S_2 \neq \emptyset$ **do**
884 $\Upsilon.\text{append}(S_2.\text{pop}())$;
885 **if** τ is not the last element in Γ **then**
886 $\Upsilon.\text{append}(\langle \text{SEP} \rangle)$;
887 prepend $\langle \text{SOS} \rangle$ and append $\langle \text{EOS} \rangle$ to Υ ;
888 **return** Υ ;

A.8 POSTFIX TRANSFORMATION CONVERSION

893 Algorithm 1 converts each feature-transformation sequence Γ written in infix form into a single
894 postfix-notation sequence Υ . We maintain a list Υ and two stacks S_1 and S_2 . For every transforma-
895 tion expression $\tau \in \Gamma$, we scan its tokens from left to right: feature ID tokens are pushed onto S_2 ,
896 left parentheses are pushed onto S_1 , operators trigger a pop from S_1 to S_2 until the top of S_1 is a left
897 parenthesis, and right parentheses trigger a pop from S_1 to S_2 until the matching left parenthesis,
898 which is discarded. After finishing one expression, we flush S_2 into Υ . Between two expressions we
899 insert a special token $\langle \text{SEP} \rangle$, and we finally wrap the whole sequence with $\langle \text{SOS} \rangle$ at the beginning
900 and $\langle \text{EOS} \rangle$ at the end.

901
902
903
904
905
906
907
908
909
910
911
912
913
914
915
916
917